Bilecik Şeyh Edebali Üniversitesi Fen Bilimleri Dergisi
Bilecik Seyh Edebali University Journal of Science
11(2), 422-436, 2024
DOİ: 10.35193/bseufbd.1360451
e-ISSN: 2458-7575 (https://dergipark.org.tr/tr/pub/bseufbd)

Araştırma Makalesi - Research Article

The Efficient Robust Conformable Methods for Solving the Conformable Fractional Cahn-Allen Equation

Uyumlu Kesirli Mertebeden Cahn-Allen Denklemini Çözmek için Etkili Uyumlu Yöntemler

Özkan Avit[1], Halil Anaç[2*]

Geliş / Received: 14/09/2023 ***Revize / Revised: 30/01/2024*** ***Kabul / Accepted: 01/03/2024***

ABSTRACT

This study focuses on the novel conformable methods employed to obtain new numerical solutions for the Cahn-Allen equation with conformable fractional derivatives. One of the two distinct methods put forth is the Cq-HATM, a hybrid technique that integrates the q-homotopy analysis transform method with the Laplace transform, utilizing the definition of conformable derivative. The CHPETM is a hybrid technique that combines the homotopy perturbation method with the Elzaki transform (ET). New numerical solutions of the conformal fractional differential Cahn-Allen equation were obtained using CHPETM and Cq-HATM. The computer simulations have been conducted in order to provide validation for the efficacy and reliability of the proposed methods. Upon performing a comparative analysis between the exact solutions and the solutions obtained through the novel methods, it becomes evident that both of these approaches exhibit simplicity, efficacy, and proficiency in addressing nonlinear conformable time-fractional coupled systems.

Keywords- Cahn-Allen equation, conformable homotopy perturbation Elzaki transform method, conformable Elzaki transform

ÖZ

Bu çalışma, uyumlu kesirli türevli Cahn-Allen denkleminin yeni sayısal çözümlerini elde etmek için kullanılan yeni uyumlu yöntemlere odaklanmaktadır. Öne sürülen iki farklı yöntemden biri, uyumlu kesirli türev tanımını kullanarak, q-homotopi analizi dönüşüm yöntemi ile Laplace dönüşümünün birleşiminden oluşan hibrit bir yöntem olan Uq-HADY' dir. UHPEDM, homotopi pertürbasyon yönteminin Elzaki dönüşümüyle birleşiminden oluşan hibrit bir yöntemdir. Uyumlu kesirli türevli Cahn-Allen denkleminin yeni nümerik çözümleri UHPEDM ve Uq-HADY kullanılarak elde edilmiştir. Önerilen metodların etkinliğinin ve güvenilirliğinin doğrulanmasını sağlamak amacıyla bilgisayar simülasyonları yapılmıştır. Kesin çözümler ile yeni yöntemlerden elde edilen çözümler arasında karşılaştırma analizi yapıldığında, bu yaklaşımların her ikisinin de doğrusal olmayan uyumlu zaman-kesirli bağlı sistemleri ele almada basitlik, etkinlik ve yeterlilik sergiledikleri ortaya çıkmaktadır.

Anahtar Kelimeler-Cahn-Allen denklemi, uyumlu homotopi pertürbasyon Elzaki dönüşüm metodu, uyumlu Elzaki dönüşümü

[1]Contact: secondauthor@example.com (https://orcid.org/XXXX-XXXX-XXXX-XXhttps://orcid.org/0009-0003-7503-1012XX)
Mathematical Engineering of Department, Gumushane University, Address Gumushane University Faculty of Engineering and Natural Sciences
[2]*Corresponding author contact: halilanac0638@gmail.com (https://orcid.org/0000-0002-1316-3947)
Computer Technologies, Gumushane University, Address Gumushane University Torul Vocational School

I. INTRODUCTION

Extensive study has been conducted in the topic of fractional calculus, leading to its formal definition by numerous esteemed scientists. The researchers have formulated novel conceptualizations of fractional calculus (FC), which subsequently laid the foundational framework for the field of fractional analysis. Fractional differential equations (FDEs) are frequently employed in the construction of nonlinear models. The utilization of FC has been utilized to analyze and explore diverse topics, such as chaos theory, financial models, disordered environments, and optics. The application of solutions generated from FDEs plays a crucial role in the discovery and understanding of nonlinear occurrences in the natural world. A diverse range of analytical and numerical methods are employed in order to get precise solutions for fractional differential equations that incorporate nonlinear phenomena, due to their inherent complexity. [1-11].

Khalil et al. have recently introduced a novel conceptualization of fractional derivative and fractional integral in their scientific publication. The authors have successfully demonstrated that the newly presented definition exhibits the fundamental characteristics of the classical derivative as described in classical analysis, while also adding a limit form that closely approaches the definition of the classical derivative. The author introduces a novel conception of the fractional derivative in their scholastic contribution. The definition presented incorporates a variety of mathematical concepts, including the product rule, quotient rule, chain rule, fractional Rolle's theorem, and fractional mean value theorems. The utilization of the conformable fractional derivative is regarded as a key and very advantageous approach. Furthermore, it increases our ability to articulate the actions exhibited by tangible entities. The utilization of the conformable fractional derivative gives an innovative approach for addressing intricate problem domains. Fractional order models are commonly employed in the field of engineering and applied sciences due to their ability to offer a more precise representation of real-world phenomena. Conformable fractional derivatives have been employed by a multitude of academics across several academic fields. The utilization of the conformable fractional operator serves as a viable approach to tackle specific limitations that are present in existing fractional operators. The subject matter being examined spans a range of mathematical concepts, such as the mean value theorem, the chain rule, the product rule for differentiating two functions, the derivative of the quotient of two functions, and Rolle's theorem [12].

The Elzaki transform method has been utilized for solving the ordinary differential equations. Differential transform method (DTM) in conjunction with ET has been employed to address a range of nonlinear differential equations. The Homotopy Perturbation Elzaki Transform Method (HPETM) was initially introduced by Elzaki and Hilal in their original work. Furthermore, the HPETM has successfully solved three nonlinear partial differential equations (PDEs). Elzaki and Kim employed a novel hybrid approach that combines the ET with the modified variational iteration method to tackle the radial diffusivity and shock wave equations in their research. Aggarwal et al. employed the method of ET to obtain solutions for the first kind Volterra integral equations. HPETM is applied to construct a solution for the fractional Navier-Stokes equations [13-18].

However, it is imperative to recognize that the fractional order has the ability to exhibit both time and space. The topic under consideration pertains to the advancing field of fractional partial differential equations (FPDEs) that encompass operators with varying orders of fractional differentiation. Numerous rigorous numerical methods have been devised and documented in scholarly publications, with substantial contributions from respected experts within the discipline. A multitude of approaches have been proposed in academic literature to tackle mathematical conundrums. This collection of techniques includes Adomian Decomposition Method (ADM), Homotopy Analysis Method (HAM), Homotopy Perturbation Method (HPM), Collocation Method, Sumudu Transform Method (STM), DTM, and Variational Iteration Method (VIM) [19-38].

Yasar and Giresunlu employed the homotopy analysis method to obtain the fractional order analytical solution to the Cahn–Allen equation (CAE) [44]. The time-fractional CAE was examined using the fractional sub-equation method to provide an approximation solution for the S-H equation [45]. Yasar et al. employed the (G'/G)-expansion method to obtain a series solution for the space-time CAE [46]. Hariharan and Kannan employed the Haar wavelet method to provide a numerical solution for the CAE [47]. Tascan and Bekir discovered both solitary and periodic wave solutions for the CAE [48]. The modified handy equation technique is utilized to provide novel feasible solutions for the CAE, and the resulting outcomes are also consistent with the penalties proposed by Tariq and Akram [49]. Bekir [50] utilized the double exp-function method to solve the CAE and obtain solutions for one-soliton and two-soliton cases. Guner et al. investigate three methods for analyzing the time-fractional order CAE [51].

The primary objective of this project is to acquire innovative numerical solutions for the Cahn-Allen equation with conformable fractional derivative (CFD). This will be achieved by employing the conformable q-homotopy analysis transform method (Cq-HATM). The secondary objective of the study is to acquire innovative numerical solutions for the Cahn-Allen equation using CFD. The objective will be accomplished by the utilization of the conformable homotopy perturbation Elzaki transform method (CHPETM).

The subsequent enumeration presents a detailed inventory of the other constituents of the study. The following section of the article provides a thorough explanation of the fundamental principles that underlie conformable fractional calculus and the Elzaki transform in Section 2. Section 3 introduces novel numerical approaches that are capable of conforming to specific requirements. Section 4 of the document presents an illustrative example of the conformable time-fractional Cahn-Allen equation. The findings are presented in Section 5.

II. PRELIMINARIES

This section presents a set of foundational definitions.

Definition 2.1. [12, 39-41] Let a function $g: [0,\infty) \to \mathbb{R}$. Then, CFD of g order α is defined as

$$T_\alpha(g)(x) = \lim_{\varepsilon \to 0} \frac{g(x + \varepsilon x^{1-\alpha}) - g(x)}{\varepsilon}, \alpha \in (0,1]. \tag{2}$$

for all $x > 0$.

Theorem 2.1. [12, 39-41] Assume that $\alpha \in (0,1]$ and The functions g and h exhibit α −differentiability at a point $x > 0$., The following conditions exist:

$$(i)\ T_\alpha(ag + bh) = aT_\alpha(g) + bT_\alpha(h), \text{for all } a, b \in \mathbb{R}, \tag{3}$$

$$(ii) T_\alpha(x^p) = px^{p-1}, \text{for all } p \in \mathbb{R}, \tag{4}$$

$$(iii) T_\alpha(\lambda) = 0, for\ all\ constant\ functions, f(t) = \lambda, \tag{5}$$

$$(iv) T_\alpha(gh) = gT_\alpha(h) + hT_\alpha(g), \tag{6}$$

$$(v) T_\alpha\left(\frac{g}{h}\right) = \frac{hT_\alpha(g) - gT_\alpha(h)}{h^2}. \tag{7}$$

Definition 2.2. [42] Assume that $\alpha \in (0,1]$, $h: [0,\infty) \to \mathbb{R}$ is function. The conformable fractional Elzaki transform (CFET) of order α of h is defined as

$${}_cE_\alpha[h(t)] = T_\alpha(v) = \int_0^\infty pK_\alpha(-p,t)h(t)d_\alpha t, \tag{8}$$

where $K_\alpha(-p,t) = E_\alpha\left(-\frac{1}{p}, t\right), p > 0$.

Definition 2.3. [42] Assume that $\alpha \in (0,1]$, $h: [0,\infty) \to \mathbb{R}$ is function. The CFET for the CFD of the function $h(t)$ is defined as

$${}_cE_\alpha[T_\alpha h(t)](p) = \frac{1}{p}\ {}_cE_\alpha[h(t)](p) - ph(0). \tag{9}$$

III. THE NOVEL NUMERICAL TECHNIQUES

This section presents an overview of Cq-HATM and CHPETM.

A. Conformable q-homotopy analysis transform method

A new method is presented. Consider the conformable time-fractional order nonlinear partial differential equation (CTFNPDE) to give the main idea of Cq-HATM:

$${}_tT_\alpha w(x,t) + Aw(x,t) + Hw(x,t) = h(x,t), t > 0, \alpha \in (n-1, n], \tag{10}$$

where A is linear, , H is nonlinear operators, $h(x,t)$ is the nonhomogeneous term, and ${}_tT_\alpha$ is a CFD of order α.

Now, by performing conformable Laplace transform (CLT) on Eq. (10) and using initial condition, then we get

$$s\mathcal{L}_\alpha[w(x,t)] - \sum_{m=0}^{k-1} w(x,0) + \mathcal{L}_\alpha[Aw(x,t)] + \mathcal{L}_\alpha[Hw(x,t)] = \mathcal{L}_\alpha[h(x,t)]. \tag{11}$$

If we simplify the Eq. (11), then we have

$$\mathcal{L}_\alpha[w(x,t)] - \frac{1}{s}w(x,0) + \frac{1}{s}\mathcal{L}_\alpha[Aw(x,t)] + \frac{1}{s}\mathcal{L}_\alpha[Hw(x,t)] - \frac{1}{s}\mathcal{L}_\alpha[h(x,t)] = 0. \tag{12}$$

We define the nonlinear operator by the assist of HAM for real function $\varphi(x,t;q)$ as follows

$$N[\varphi(x,t;q)\,] = \mathcal{L}_\alpha[\varphi(x,t;q)\,] - \frac{1}{s}\varphi(x,t;q)\,(0^+) + \frac{1}{s}(\mathcal{L}_\alpha[A\varphi(x,t;q)] + \mathcal{L}_\alpha[H\varphi(x,t;q)]$$

$$-\mathcal{L}_\alpha[h(x,t)]), \tag{13}$$

where $q\epsilon\left[0,\frac{1}{n}\right]$.

We establish a homotopy in the following:

$$(1-nq)\mathcal{L}_\alpha[\varphi(x,t;q) - w_0(x,t)] = hqH^+(x,t)H[\varphi(x,t;q)], \tag{14}$$

where, $h \neq 0$ is an auxiliary parameter and $\mathcal{L}_\alpha$ demonstrates conformable Laplace transform. For $q = 0$ and $q = \frac{1}{n}$, the outcomes in Eq. (14) are respectively provided:

$$\varphi(x,t;0) = w_0(x,t), \varphi\left(x,t;\frac{1}{n}\right) = w(x,t). \tag{15}$$

Hence, by incrementing q from 0 to $\frac{1}{n}$, then the solution $\varphi(x,t;q)$ converges from $w_0(x,t)$ to the solution $w(x,t)$. Employing the Taylor theorem around q and expanding $\varphi(x,t;q)$ and then, we obtain

$$\varphi(x,t;q) = w_0(x,t) + \sum_{i=1}^{\infty} w_m(x,t)q^m, \tag{16}$$

where

$$w_m(x,t) = \frac{1}{m!}\frac{\partial^m\varphi(x,t;q)}{\partial q^m}|_{q=0}. \tag{17}$$

Eq. (16) converges at $q = \frac{1}{n}$ for the appropriate $w_0(x,t)$, n and h. Then, we have

$$w(x,t) = w_0(x,t) + \sum_{m=1}^{\infty} w_m(x,t)\left(\frac{1}{n}\right)^m. \tag{18}$$

If we differentiate the zeroth order deformation Eq. (14) m −times with respect to q and we divide by $m!$, respectively, then for $q = 0$, we obtain

$$\mathcal{L}_\alpha[w_m(x,t) - k_m w_{m-1}(x,t)] = hH^+(x,t)\mathcal{R}_m(\vec{w}_{m-1}), \tag{19}$$

where the vectors are defined by

$$\vec{w}_m = \{w_0(x,t), w_1(x,t), \dots, w_m(x,t)\}. \tag{20}$$

When we apply to the inverse CLT to Eq. (19), then we obtain

$$w_m(x,t) = k_m w_{m-1}(x,t) + h\mathcal{L}_\alpha{}^{-1}[H^+(x,t)\mathcal{R}_m(\vec{w}_{m-1})], \tag{21}$$

where

$$\mathcal{R}_m(\vec{w}_{m-1}) = \mathcal{L}_\alpha[w_{m-1}(x,t)] - \left(1-\frac{k_m}{n}\right)\frac{1}{s}w_0(x,t) + \frac{1}{s}\mathcal{L}_\alpha(Aw_{m-1}(x,t) + H^+_{m-1}(x,t)$$

$$-h(x,t)\Big), \tag{22}$$

and

$$k_m = \begin{cases} 0, & m \le 1, \\ n, & m > 1. \end{cases} \tag{23}$$

where, H_m^+ is homotopy polynomial and presented as

$$H_m^+ = \frac{1}{m!}\frac{\partial^m \varphi(x,t;q)}{\partial q^m}|_{q=0} \quad \text{and } \varphi(x,t;q) = \varphi_0 + q\varphi_1 + q^2\varphi_2 + \cdots. \tag{24}$$

By utilizing Eqs. (21)-(22),then we obtain

$$w_m(x,t) = (k_m + h)w_{m-1}(x,t) - \left(1-\frac{k_m}{n}\right)\frac{1}{s}w_0(x,t) + \mathrm{h}\mathcal{L}_\alpha{}^{-1}\left[\left(\frac{1}{s}\mathcal{L}_\alpha[Rw_{m-1}(x,t)\right.\right.$$

$$\left.\left.+H_{m-1}(x,t) - f(x,t)]\right)\right]. \tag{25}$$

By using q-HATM, the series solution is

$$w(x,t) = \sum_{m=0}^{\infty} w_m(x,t)\left(\frac{1}{n}\right)^m. \tag{26}$$

III. CONFORMABLE ELZAKI ADOMIAN DECOMPOSITION METHOD

The analysis of the CTFNPDE in Eq. (10) is performed.

Now, by performing conformable Elzaki transform (CET) on Eq. (10) and using initial condition, then we have

$$\frac{1}{v}\,{}_cE_\alpha[w(x,t)] - vw(x,0) + {}_cE_\alpha[Aw(x,t) + Hw(x,t)] = {}_cE_\alpha[h(x,t)]. \tag{27}$$

If we simplify the Eq. (27), then we get

$${}_cE_\alpha[w(x,t)] = v^2w(x,0) + v\,{}_cE_\alpha[h(x,t)] - v\,{}_cE_\alpha[Aw(x,t) + Hw(x,t)]. \tag{28}$$

On applying inverse CET to Eq. (28), then we have

$$w(x,t) = C(x,t) - \left({}_cE_\alpha\right)^{-1}\{v\,{}_cE_\alpha[Aw(x,t) + Hw(x,t)]\}. \tag{29}$$

Now, HPM is utilized, then it is obtained as

$$w(x,t) = \sum_{n=0}^{\infty} p^n w_n(x,t). \tag{30}$$

Also, the nonlinear term has been decomposed as

$$Hw(x,t) = \sum_{n=0}^{\infty} p^n H_n(w), \tag{31}$$

where the homotopy polynomial $H_n(w)$ is given by

$$H_n(w_0, w_1, \dots, w_n) = \frac{1}{n!}\frac{\partial}{\partial p^n}\left[H\left(\sum_{i=0}^{\infty} p^i w_i\right)\right]_{p=0}, n = 0,1,2,\dots \tag{32}$$

Eqs. (30)-(31) are substituted in Eq. (29), then we have

$$\sum_{n=0}^{\infty} p^n w_n(x,t) = G(x,t) - p\left\{(E_\alpha^c)^{-1}\left\{v^2 E_\alpha^c\left[A\sum_{n=0}^{\infty} p^n w_n(x,t) + \sum_{n=0}^{\infty} p^n H_n(w)\right]\right\}\right\} \tag{33}$$

where $G(x,t)$ is the term consisting of the initial condition and the external source term.

If we compare the identical powers of p, the resulting iterations are as follows:

$$\begin{aligned} p^0&: w_0(x,t) = G(x,t), \\ p^1&: w_1(x,t) = -E^{-1}\{v^2 E[Aw_0(x,t) + H_0(w)]\} \\ p^2&: w_2(x,t) = -E^{-1}\{v^2 E[Aw_1(u,t) + H_1(w)]\} \\ p^3&: w_3(x,t) = -E^{-1}\{v^2 E[Aw_2(u,t) + H_2(w)]\} \\ &\vdots \end{aligned} \tag{34}$$

Ultimately, the solution $u(x,t)$ is approximated as follows.

$$w(x,t) = \lim_{p\to 1}\sum_{n=0}^{\infty} p^n w_n(x,t) = w_0(x,t) + w_1(x,t) + w_2(x,t) + \cdots \tag{35}$$

IV. RESULTS

This section seeks to provide graphic depictions of the conformable time-fractional Cahn-Allen equation.

Example 3.1. [43] Consider the conformable time-fractional Cahn-Allen equation (CTFCAE)

$$\{\ D_t^\alpha w(x,t) - w_{xx}(x,t) + w^3(x,t) - w(x,t) = 0\ ,\qquad t > 0,\qquad 0 < \alpha \le 1 \tag{36}$$

with the initial conditions

$$w(x,0) = \frac{1}{1 + e^{\frac{-x}{\sqrt{2}}}}. \tag{37}$$

Case (i) Cq-HATM solution

CLT is employed to Eq. (37), and by applying Eq. (38), the resulting expression is produced as

$$\mathcal{L}_\alpha[w(x,t)] - \frac{1}{s}w(x,0) + \frac{1}{s}\mathcal{L}_\alpha[-w_{xx} + w^3 - w] = 0. \tag{38}$$

The nonlinear operators are defined by employing Eq. (38):

$$N[\varphi(x,t;q)] = \mathcal{L}_\alpha[\varphi(x,t;q)] - \frac{1}{s}\left(\frac{1}{1+e^{\frac{-x}{\sqrt{2}}}}\right) + \frac{1}{s}\mathcal{L}_\alpha\left[-\frac{\partial^2\varphi(x,t;q)}{\partial x^2} + \varphi^3(x,t;q) - \varphi(x,t;q)\right]. \tag{39}$$

The $m-th$ order deformation equations are defined by the application of the proposed algorithm:

$$\mathcal{L}_\alpha[w_m(x,t) - k_m w_{m-1}(x,t)] = h\mathcal{R}_m(w_{m-1}), \tag{40}$$

where

$$\mathcal{R}_m(w_{m-1}) = \mathcal{L}_\alpha[w_{m-1}] - \frac{1}{s}\left(1-\frac{k_m}{n}\right).\left(\frac{1}{1+e^{\frac{-x}{\sqrt{2}}}}\right)$$

$$+\frac{1}{s}\mathcal{L}_\alpha\left[-\frac{\partial^2 w_{m-1}}{\partial x^2} + \sum_{r=0}^{m-1}\left(\sum_{j=0}^{r} w_j.w_{r-j}\right)w_{m-1-r} - w_{m-1}\right]. \tag{41}$$

By utilizing the inverse CLT to Eq. (40), we obtain

$$w_m = k_m w_{m-1} + h\mathcal{L}_\alpha{}^{-1}[\mathcal{R}_m(w_{m-1})]. \tag{42}$$

By employing initial conditions, we are able to drive

$$w_0(x,t) = \frac{1}{1+e^{\frac{-x}{\sqrt{2}}}}, \tag{43}$$

To get the value of $w_1(x,t)$, we substitute $m=1$ into Eq. (42), resulting in the following expression:

$$w_1(x,t) = h\left(\frac{-3e^{\frac{-x\sqrt{2}}{2}}}{2\left(1+e^{\frac{-x\sqrt{2}}{2}}\right)^2}\right)\frac{t^\alpha}{\alpha}, \tag{44}$$

In a similar vein, by substituting $m=2$ into Eq. (42), the resulting value for $w_2(x,t)$ can be obtained:

$$w_2(x,t) = (n+h)w_1 + h\frac{t^{2\alpha}}{8\alpha^2}\frac{9\left(e^{\frac{-x\sqrt{2}}{2}}-1\right)he^{\frac{-x\sqrt{2}}{2}}}{2\left(1+e^{\frac{-x\sqrt{2}}{2}}\right)^3}. \tag{45}$$

Similarly, by substituting $m=3$ into Eq. (42), the resulting value for $w_3(x,t)$ can be obtained:

$$w_3(x,t) = (n+h)w_2 - 27h^2\frac{e^{\frac{-x\sqrt{2}}{2}}}{16\alpha^2(1+e^{\frac{-x\sqrt{2}}{2}})^4}$$

$$+\left[\frac{-4(n+h)\left(e^{-x\sqrt{2}}-1\right)t^{2\alpha}}{6} + \left(e^{-x\sqrt{2}} - 4e^{\frac{-x\sqrt{2}}{2}} + 1\right)h\frac{t^{3\alpha}}{3\alpha}\right]. \tag{46}$$

By employing this approach, it is possible to identify the remaining terms. The solutions of the CTFCAE are determined through the Cq-HATM:

$$w(x,t) = w_0(x,t) + \sum_{m=1}^{\infty} w_m(x,t)\left(\frac{1}{n}\right)^m. \tag{47}$$

By substituting $\alpha = 1, n = 1,\ h = -1$ into Eq. (47), we have that the resulting outcome, denoted as $\sum_{m=1}^{M} w_m(x,t)\left(\frac{1}{n}\right)^m$ to the exact solution $w(x,t) = \frac{1}{1+e^{\left(\frac{-x\sqrt{2}}{2} \frac{3t}{2}\right)}}$ of the CTFCAE when $M \to \infty$.

Case (ii) CHPEDM solution

By employing the CET to Eq. (36) and utilizing Eq. (37), the resulting expression is obtained.

$$\frac{1}{s}E_\alpha^c[w(x,t)] - sw(x,0) + E_\alpha^c[-w_{xx} + w^3 - w] = 0, \tag{48}$$

Rearranging Eq. (48), then we obtain

$$E_\alpha^c[w(x,t)] = s^2 \frac{1}{1+e^{\frac{-x}{\sqrt{2}}}} - sE_\alpha[-w_{xx} + w^3 - w], \tag{49}$$

By utilizing the inverse CET on Eq. (48), we are able to derive the following result:

$$w(x,t) = \frac{1}{1+e^{\frac{-x}{\sqrt{2}}}} - (E_\alpha^c)^{-1}\left[sE_\alpha^c[-w_{xx} + w^3 - w]\right], \tag{50}$$

Let us consider the assumption that the answer to the infinite series can be expressed in the following form:

$$w(x,t) = \sum_{m=0}^{\infty} w_m(x,t). \tag{51}$$

Utilizing HPM, now, if we rewrite Eq. (50), then it is obtained as

$$\begin{aligned}\sum_{m=0}^{\infty} p^m w_m(x,t) &= \left(\frac{1}{1+e^{\frac{-x}{\sqrt{2}}}}\right) \\ &+ p\left\{E_\alpha^{-1}\left[sE_\alpha\left(-\sum_{m=0}^{\infty} p^m (w_m)_{xx} + \sum_{m=0}^{\infty} p^m H_m(w) - \sum_{m=0}^{\infty} p^m w_m\right)\right]\right\},\end{aligned} \tag{52}$$

The symbols $H_m(w)$ represent He's polynomials, that are utilized to represent nonlinear variables.

Some components of $H_m(w)$ are as follows.

$$H_0(w) = {w_0}^3, \tag{53}$$

$$H_1(w) = 3{w_0}^3 w_1, \tag{54}$$

$$H_2(w) = 3{w_0}^3 w_2 + 3{w_1}^2 w_0, \tag{55}$$

If the powers of p are compared, they are obtained in the same manner.

$$p^0: w_0(x,t) = 1 + e^{\frac{-x}{\sqrt{2}}}, \qquad H_0(w) = (1 + e^{\frac{-x}{\sqrt{2}}})^3, \tag{56}$$

$$p^1: w_1(x,t) = \frac{3e^{\frac{-x\sqrt{2}}{2}}t^\alpha}{2\alpha\left(1 + e^{\frac{-x\sqrt{2}}{2}}\right)^2}, \qquad H_1(w) = \frac{3(1 + e^{\frac{-x}{\sqrt{2}}})^2.3e^{\frac{-x\sqrt{2}}{2}}t^\alpha}{2(1 + e^{\frac{-x\sqrt{2}}{2}})^2\alpha}, \tag{57}$$

$$p^2: w_2(x,t) = \frac{9(e^{\frac{-x\sqrt{2}}{2}} - 1)t^\alpha e^{\frac{-x\sqrt{2}}{2}}}{8\alpha^2(1 + e^{\frac{-x\sqrt{2}}{2}})^3}, H_2(w) = \frac{27e^{\frac{-x\sqrt{2}}{2}}(3e^{\frac{-x\sqrt{2}}{2}} - 1)t^{2\alpha}}{8\alpha^2(1 + e^{\frac{-x\sqrt{2}}{2}})^5}, \tag{58}$$

By continuing in a similar manner, the outcomes for CTFCAE can be derived.

$$w(x,t) = \sum_{m=0}^{\infty} w_m(x,t) = w_0(x,t) + w_1(x,t) + w_2(x,t) + \cdots$$

$$= 1 + e^{\frac{-x}{\sqrt{2}}} + \frac{3e^{\frac{-x\sqrt{2}}{2}}t^\alpha}{2\alpha\left(1 + e^{\frac{-x\sqrt{2}}{2}}\right)^2} + \frac{9(e^{\frac{-x\sqrt{2}}{2}} - 1)t^\alpha e^{\frac{-x\sqrt{2}}{2}}}{8\alpha^2(1 + e^{\frac{-x\sqrt{2}}{2}})^3}. \tag{59}$$

Fig. 1 displays the 3D graphical representations of Cq-HATM, the exact solution, and the absolute error for $w(x,t)$.

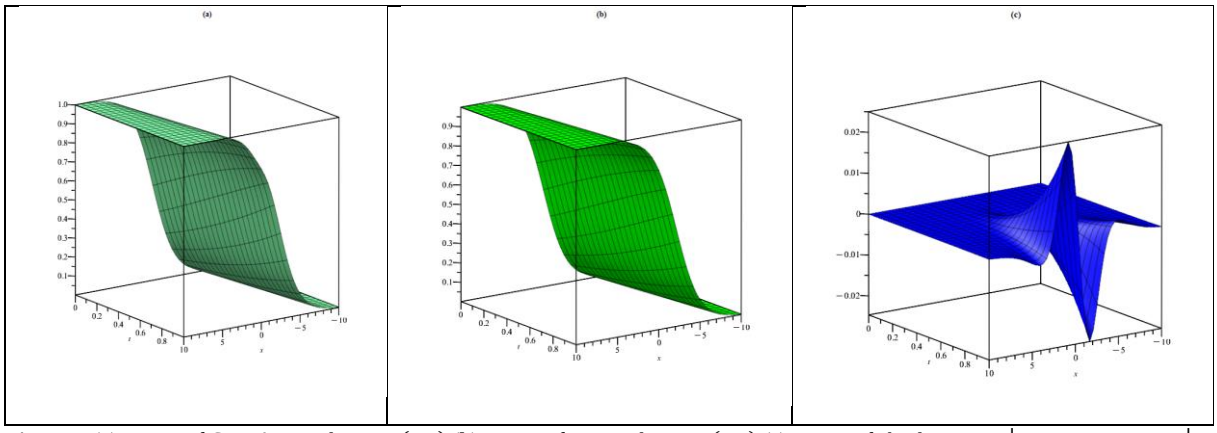

Figure 1. (a) Nature of Cq-HATM solution $w(x,t)$ **(b)** Nature of exact solution $w(x,t)$ **(c)** Nature of absolute error=$\left|w_{exact} - w_{Cq-HATM}\right|$ at $h = -1, n = 1, \alpha = 1$ for CTFCAE.

Fig. 2 presents the three-dimensional graphical depictions of CHPETM, the exact solution, and the absolute error for $w(x,t)$.

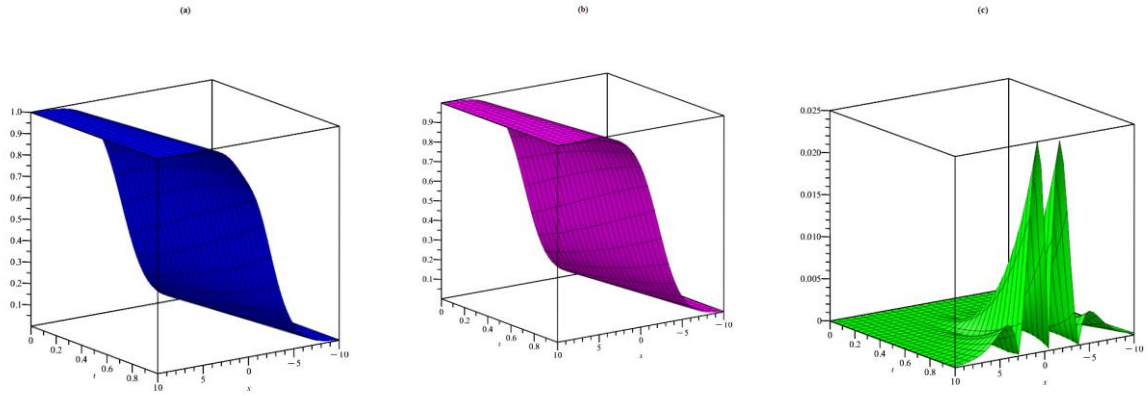

Figure 2. (a) Nature of CHPETM solution $w(x,t)$ **(b)** Nature of exact solution $w(x,t)$ **(c)** Nature of absolute error=$|w_{exact} - w_{CHPETM}|$ at $\alpha = 1$ for CTFCAE.

Figure 3 shows the two-dimensional graphical representations of Cq-HATM and CHPETM for $w(x,t)$ solutions for different α values.

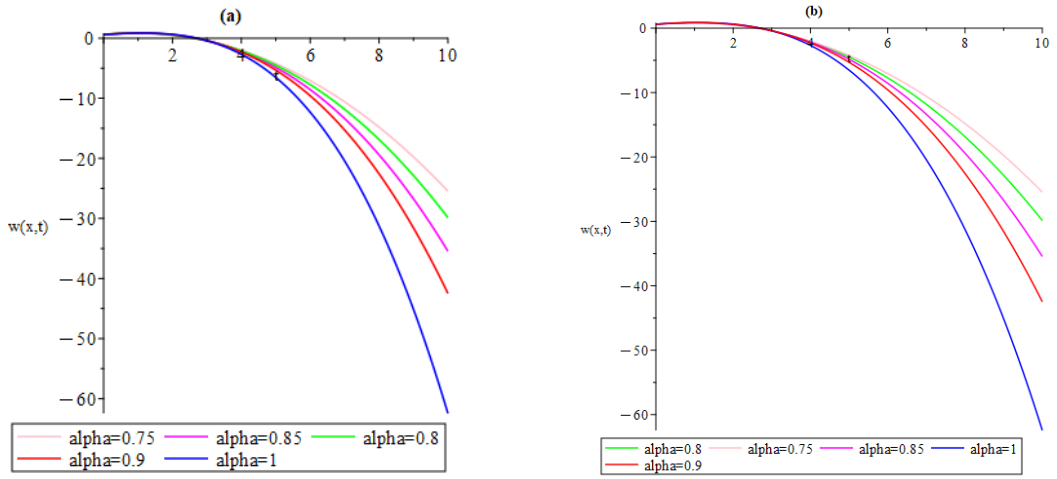

Figure 3. The comparison of the Cq-HATM solutions for $w(x,t)$ **(b)** The comparison of the CHPETM solutions for $w(x,t)$ at $h = -1, n = 1, x = 0.5$ with different α.

Table 1 shows the numerical solutions of w(x, t) obtained from the solution of CTFCAE with Cq-HATM for different x, t and α values.

Table 1. *Numerical solution of $w(x,t)$ by Cq-HATM for CTFCAE with different x, t and α at $n = 1, h = -1$.*

x	t	$\alpha = 0.75$	$\alpha = 0.8$	$\alpha = 0.85$	$\alpha = 0.9$	$\alpha = 1$
1	0.001	2.1×10^{-3}	1.3×10^{-3}	7.6×10^{-4}	4.0×10^{-4}	1.4×10^{-10}
	0.002	3.5×10^{-3}	2.2×10^{-3}	1.3×10^{-3}	7.0×10^{-4}	7.1×10^{-11}
	0.003	4.6×10^{-3}	2.9×10^{-3}	1.7×10^{-3}	9.7×10^{-4}	1.3×10^{-10}
	0.004	5.6×10^{-3}	3.6×10^{-3}	2.2×10^{-3}	1.2×10^{-3}	4.7×10^{-11}
	0.005	6.6×10^{-3}	4.2×10^{-3}	2.6×10^{-3}	1.4×10^{-3}	2.1×10^{-10}
2	0.001	1.5×10^{-3}	9.3×10^{-4}	5.4×10^{-4}	2.8×10^{-4}	1.3×10^{-10}
	0.002	2.4×10^{-3}	1.5×10^{-3}	9.3×10^{-4}	5.0×10^{-4}	1.0×10^{-10}
	0.003	3.2×10^{-3}	2.1×10^{-3}	1.2×10^{-3}	6.9×10^{-4}	1.9×10^{-10}
	0.004	4.0×10^{-3}	2.5×10^{-3}	1.5×10^{-3}	8.7×10^{-4}	2.7×10^{-10}
	0.005	4.6×10^{-3}	3.0×10^{-3}	1.8×10^{-3}	1.0×10^{-3}	1.9×10^{-10}
3	0.001	9.2×10^{-4}	5.6×10^{-4}	3.3×10^{-4}	1.7×10^{-4}	2.3×10^{-15}
	0.002	1.5×10^{-3}	9.4×10^{-4}	5.6×10^{-4}	3.0×10^{-4}	3.7×10^{-14}
	0.003	1.9×10^{-3}	1.2×10^{-3}	7.7×10^{-4}	4.2×10^{-4}	1.8×10^{-13}
	0.004	2.4×10^{-3}	1.5×10^{-3}	9.6×10^{-4}	5.2×10^{-4}	5.9×10^{-13}
	0.005	2.8×10^{-3}	1.8×10^{-3}	1.1×10^{-3}	6.3×10^{-4}	1.4×10^{-12}
4	0.001	5.1×10^{-4}	3.1×10^{-4}	1.8×10^{-4}	9.5×10^{-5}	3.6×10^{-15}
	0.002	8.3×10^{-4}	5.2×10^{-4}	3.1×10^{-4}	1.6×10^{-4}	5.8×10^{-14}
	0.003	1.0×10^{-3}	7.0×10^{-4}	4.2×10^{-4}	2.3×10^{-4}	2.9×10^{-13}
	0.004	1.3×10^{-3}	8.6×10^{-4}	5.3×10^{-4}	2.9×10^{-4}	9.3×10^{-13}
	0.005	1.5×10^{-3}	1.0×10^{-3}	6.2×10^{-4}	3.4×10^{-4}	2.2×10^{-12}

5	0.001	2.6×10^{-4}	1.6×10^{-4}	9.5×10^{-5}	5.0×10^{-5}	3.6×10^{-15}
	0.002	4.3×10^{-4}	2.7×10^{-4}	1.6×10^{-4}	8.7×10^{-5}	5.8×10^{-14}
	0.003	5.7×10^{-4}	3.6×10^{-4}	2.2×10^{-4}	1.2×10^{-4}	2.9×10^{-13}
	0.004	6.9×10^{-4}	4.5×10^{-4}	2.7×10^{-4}	1.5×10^{-4}	9.3×10^{-13}
	0.005	8.1×10^{-4}	5.2×10^{-4}	3.2×10^{-4}	1.8×10^{-4}	2.2×10^{-12}

Table 2 presents the numerical solution of the function $w(x,t)$, which was derived from the solution of the CTFCAE using the CHPETM. The table displays the results for various values of x, t, and α.

Table 2. *Numerical solution of $w(x,t)$ by CHPETM for CTFCAE with different x, t and α.*

x	t	$\alpha = 0.75$	$\alpha = 0.8$	$\alpha = 0.85$	$\alpha = 0.9$	$\alpha = 1$
1	0.001	2.1×10^{-3}	1.3×10^{-3}	7.6×10^{-4}	4.0×10^{-4}	1.4×10^{-10}
	0.002	3.5×10^{-3}	2.2×10^{-3}	1.3×10^{-3}	7.0×10^{-4}	7.1×10^{-11}
	0.003	4.6×10^{-3}	2.9×10^{-3}	1.7×10^{-3}	9.7×10^{-4}	1.3×10^{-10}
	0.004	5.6×10^{-3}	3.6×10^{-3}	2.2×10^{-3}	1.2×10^{-3}	4.7×10^{-11}
	0.005	6.6×10^{-3}	4.2×10^{-3}	2.6×10^{-3}	1.4×10^{-3}	2.1×10^{-10}
2	0.001	1.5×10^{-3}	9.3×10^{-4}	5.4×10^{-4}	2.8×10^{-4}	1.3×10^{-10}
	0.002	2.4×10^{-3}	1.5×10^{-3}	9.3×10^{-4}	5.0×10^{-4}	1.0×10^{-10}
	0.003	3.2×10^{-3}	2.1×10^{-3}	1.2×10^{-3}	6.9×10^{-4}	1.9×10^{-10}
	0.004	4.0×10^{-3}	2.5×10^{-3}	1.5×10^{-3}	8.7×10^{-4}	2.7×10^{-10}
	0.005	4.6×10^{-3}	3.0×10^{-3}	1.8×10^{-3}	1.0×10^{-3}	1.9×10^{-10}
3	0.001	9.2×10^{-4}	5.6×10^{-4}	3.3×10^{-4}	1.7×10^{-4}	2.3×10^{-15}
	0.002	1.5×10^{-3}	9.4×10^{-4}	5.6×10^{-4}	3.0×10^{-4}	3.7×10^{-14}
	0.003	1.9×10^{-3}	1.2×10^{-3}	7.7×10^{-4}	4.2×10^{-4}	1.8×10^{-13}
	0.004	2.4×10^{-3}	1.5×10^{-3}	9.6×10^{-4}	5.2×10^{-4}	5.9×10^{-13}
	0.005	2.8×10^{-3}	1.8×10^{-3}	1.1×10^{-3}	6.3×10^{-4}	1.4×10^{-12}
4	0.001	5.1×10^{-4}	3.1×10^{-4}	1.8×10^{-4}	9.5×10^{-5}	3.6×10^{-15}
	0.002	8.3×10^{-4}	5.2×10^{-4}	3.1×10^{-4}	1.6×10^{-4}	5.8×10^{-14}
	0.003	1.0×10^{-3}	7.0×10^{-4}	4.2×10^{-4}	2.3×10^{-4}	2.9×10^{-13}
	0.004	1.3×10^{-3}	8.6×10^{-4}	5.3×10^{-4}	2.9×10^{-4}	9.3×10^{-13}
	0.005	1.5×10^{-3}	1.0×10^{-3}	6.2×10^{-4}	3.4×10^{-4}	2.2×10^{-12}
5	0.001	2.6×10^{-4}	1.6×10^{-4}	9.5×10^{-5}	5.0×10^{-5}	3.6×10^{-15}
	0.002	4.3×10^{-4}	2.7×10^{-4}	1.6×10^{-4}	8.7×10^{-5}	5.8×10^{-14}
	0.003	5.7×10^{-4}	3.6×10^{-4}	2.2×10^{-4}	1.2×10^{-4}	2.9×10^{-13}
	0.004	6.9×10^{-4}	4.5×10^{-4}	2.7×10^{-4}	1.5×10^{-4}	9.3×10^{-13}
	0.005	8.1×10^{-4}	5.2×10^{-4}	3.2×10^{-4}	1.8×10^{-4}	2.2×10^{-12}

Table 3 shows the comparison of absolute errors of Cq-HATM, CHPETM and NITM.

Table 3. *Absolute errors obtained with Cq-HATM and CHPETM compared to NITM [43] for CTFCAE when α=1.*

x	t	$NITM$ [43]	$Cq-HATM$	$CHPETM$
1	0.001	3.3×10^{-11}	2.6×10^{-14}	2.6×10^{-14}
	0.002	2.6×10^{-10}	4.1×10^{-13}	4.1×10^{-13}
	0.003	8.9×10^{-10}	2.1×10^{-12}	2.1×10^{-12}
	0.004	2.1×10^{-9}	6.7×10^{-12}	6.7×10^{-12}
	0.005	4.1×10^{-9}	1.6×10^{-11}	1.6×10^{-11}
2	0.001	4.9×10^{-11}	1.7×10^{-14}	1.7×10^{-14}
	0.002	3.9×10^{-10}	2.8×10^{-13}	2.8×10^{-13}
	0.003	1.3×10^{-9}	1.4×10^{-12}	1.4×10^{-12}
	0.004	3.1×10^{-9}	4.5×10^{-12}	4.5×10^{-12}
	0.005	6.2×10^{-9}	1.1×10^{-11}	1.1×10^{-11}
3	0.001	4.1×10^{-11}	2.3×10^{-15}	2.3×10^{-15}
	0.002	3.3×10^{-10}	3.7×10^{-14}	3.7×10^{-14}
	0.003	1.1×10^{-9}	1.8×10^{-13}	1.8×10^{-13}
	0.004	2.6×10^{-9}	5.9×10^{-13}	5.9×10^{-13}
	0.005	5.1×10^{-9}	1.4×10^{-12}	1.4×10^{-12}
4	0.001	2.6×10^{-11}	3.6×10^{-15}	3.6×10^{-15}
	0.002	2.0×10^{-10}	5.8×10^{-14}	5.8×10^{-14}
	0.003	7.0×10^{-10}	2.9×10^{-13}	2.9×10^{-13}
	0.004	1.6×10^{-9}	9.3×10^{-13}	9.3×10^{-13}
	0.005	3.2×10^{-9}	2.2×10^{-12}	2.2×10^{-12}
5	0.001	1.4×10^{-11}	3.6×10^{-15}	3.6×10^{-15}
	0.002	1.1×10^{-10}	5.8×10^{-14}	5.8×10^{-14}
	0.003	3.9×10^{-10}	2.9×10^{-13}	2.9×10^{-13}

0.004	9.3×10^{-10}	9.3×10^{-13}	9.3×10^{-13}
0.005	1.8×10^{-9}	2.2×10^{-12}	2.2×10^{-12}

V. RESULTS AND DISCUSSION

Figure 1 exhibits the three-dimensional representations of the numerical solutions acquired by the Cq-HATM, alongside the exact solutions and the absolute errors between the Cq-HATM solutions and the exact solutions for the CTFCAE. Figure 2 exhibits the graphical representations in three dimensions that illustrate the numerical solutions acquired by the CHPETM for the CTFCAE. Furthermore, the figure 2 also presents the exact solutions and the absolute errors between the CHPETM solutions and the exact solutions. Figure 3 shows the 2D comparison of the solutions obtained with methods Cq-HATM and CHPETM for the CTFCAE. Table 1 displays the numerical solutions of w(x,t) obtained using Cq-HATM for several values of α, specifically $\alpha = 0.75, \alpha = 0.8, \alpha = 0.85, \alpha = 0.9$, and $\alpha = 1$, for CTFCAE. In addition, Table 2 presents the numerical solutions of $w(x,t)$ acquired through the use of CHPETM for various values of α, namely $\alpha = 0.75, \alpha = 0.8, \alpha = 0.85, \alpha = 0.9$, and $\alpha = 1$, for CTFCAE. Table 3 presents the absolute errors of the NITM solutions in the literature, Cq-HATM solutions and CHPETM solutions for the CTFCAE. Table 3 demonstrates that the two recently developed methods exhibit lower errors compared to NITM.

VI. CONCLUSION

This work investigates the CTFCAE using two novel numerical approaches, specifically Cq-HATM and CHPETM. The numerical findings have provided confirmation of the reliability of these newly developed methods. The newly introduced techniques for addressing nonlinear fractional partial differential equations have been found to hold significant benefits and exhibit a high level of efficacy.

REFERENCES

[1] Liouville J. (1832). Mémoire sur quelques questions de géométrie et de mécanique, et sur un nouveau genre de calcul pour résoudre ces questions. *Ecole polytechnique, 13*, 71-162.

[2] Miller, K. S., Ross, B. (1993). An introduction to the fractional calculus and fractional differential equations, Wiley, New York.

[3] Podlubny, I. (1999). Fractional differential equations, mathematics in science and engineering, Academic Press, New York.

[4] Baleanu, D., Diethelm, K., Scalas, E., Trujillo, J. J. (2012). *Fractional calculus: models and numerical methods*, World Scientific, London.

[5] Povstenko, Y. (2015). Linear fractional diffusion-wave equation for scientists and engineers. Birkhäuser, Switzerland.

[6] Baleanu D., Wu G.C., Zeng S.D. (2017). Chaos analysis and asymptotic stability of generalized Caputo fractional differential equations. *Chaos Solitons Fractals, 102*, 99–105.

[7] Sweilam, N. H., Abou Hasan, M. M., Baleanu, D. (2017). New studies for general fractional financial models of awareness and trial advertising decisions. *Chaos, Solitons & Fractals, 10*4, 772-784.

[8] Liu D. Y., Gibaru O., Perruquetti W., Laleg-Kirati T. M. (2015). Fractional order differentiation by integration and error analysis in noisy environment. *IEEE Transactions on Automatic Control, 60,* 2945–2960.

[9] Esen A., Sulaiman T.A., Bulut H., Baskonus H. M. (2018). Optical solitons to the space-time fractional (1+1)-dimensional coupled nonlinear Schrödinger equation. *Optik, 167*, 150–156.

[10] Caponetto R., Dongola G., Fortuna L., Gallo A. (2010). New results on the synthesis of FO-PID controllers. *Communications in Nonlinear Science and Numerical Simulation, 15*, 997–1007.

[11] Veeresha, P., Prakasha, D.G., Baskonus, H. M. (2019). Novel simulations to the time-fractional Fisher's equation. *Mathematical Sciences, 13*(1), 33-42.

[12] Khalil, R., Al Horani, M., Yousef, A., Sababheh, M. (2014). A new definition of fractional derivative. *Journal of computational and applied mathematics, 264*, 65-70.

[13] Aggarwal, S., Chauhan, R., Sharma, N. (2018). Application of Elzaki transform for solving linear Volterra integral equations of first kind. *International Journal of Research in Advent Technology, 6*(12), 3687-3692.

[14] Elzaki, T. M. (2011). Applications of new transform "Elzaki transform" to partial differential equations. *Global Journal of Pure and Applied Mathematics, 7*(1), 65-70.

[15] Elzaki, T. M. (2012). Solution of nonlinear differential equations using mixture of Elzaki transform and differential transform method. *In International Mathematical Forum, 7*(13), 631-638.

[16] Elzaki, T. M., Hilal, E. M. A. (2012). Homotopy perturbation and Elzaki transform for solving nonlinear partial differential equations. *Mathematical Theory and Modeling, 2*(3), 33-42.

[17] Elzaki, T. M., Kim, H. (2015). The solution of radial diffusivity and shock wave equations by Elzaki variational iteration method. *International Journal of Mathematical Analysis, 9*(22), 1065-1071.

[18] Jena, R. M., Chakraverty, S. (2019). Solving time-fractional Navier–Stokes equations using homotopy perturbation Elzaki transform. *SN Applied Sciences, 1*(1), 1-16.

[19] Abu-Gdairi, R., Al-Smadi, M., Gumah, G. (2015). An expansion iterative technique for handling fractional differential equations using fractional power series scheme. *Journal of Mathematics and Statistics, 11*(2), 29–38.

[20] Baleanu, D., Golmankhaneh, A. K., Baleanu, M. C. (2009). Fractional electromagnetic equations using fractional forms. *International Journal of Theoretical Physics, 48*(11), 3114–3123.

[21] Baleanu, D., Jajarmi, A., Hajipour, M. (2018). On the nonlinear dynamical systems within the generalized fractional derivatives with Mittag–Leffler kernel. *Nonlinear Dynamics, 2018*(1), 1–18.

[22] Baleanu, D., Asad, J. H., Jajarmi, A. 2018. New aspects of the motion of a particle in a circular cavity. *Proceedings of the Romanian Academy Series A, 19*(2), 143–149.

[23] Baleanu, D., Jajarmi, A., Bonyah, E., Hajipour, M. (2018). New aspects of poor nutrition in the life cycle within the fractional calculus. *Advances in Difference Equations, 2018*(1), 1-14.

[24] Anaç, H., Merdan, M., Bekiryazıcı, Z., Kesemen, T. (2019). Bazı Rastgele Kısmi Diferansiyel Denklemlerin Diferansiyel Dönüşüm Metodu ve Laplace-Padé Metodu Kullanarak Çözümü. *Gümüşhane Üniversitesi Fen Bilimleri Enstitüsü Dergisi, 9*(1), 108-118.

[25] Ayaz, F. (2004). Solutions of the system of differential equations by differential transform method. *Applied Mathematics and Computation, 147*(2), 547-567.

[26] He, J. H. (1999). Variational iteration method-a kind of non-linear analytical technique: some examples. *International Journal of Non-linear Mechanics, 34*(4), 699-708.

[27] He, J. H. (2003). Homotopy perturbation method: a new nonlinear analytical technique. *Applied Mathematics and Computation, 135*(1), 73-79.

[28] He, J. H. (2006). Homotopy perturbation method for solving boundary value problems. *Physics Letters, 350*(1-2), 87-88.

[29] He, J. H. (2006). Addendum: new interpretation of homotopy perturbation method. *International Journal of Modern Physics B, 20*(18), 2561-2568.

[30] Jajarmi, A., Baleanu, D. (2018). Suboptimal control of fractional-order dynamic systems with delay argument. *Journal of Vibration and Control, 24*(12), 2430-2446.

[31] Jajarmi, A., Baleanu, D. (2018). A new fractional analysis on the interaction of HIV with CD4+ T-cells, *Chaos, Solitons & Fractals, 113*, 221-229.

[32] Kangalgil, F., Ayaz, F. (2009). Solitary wave solutions for the KdV and mKdV equations by differential transform method. *Chaos, Solitons & Fractals*, *41*(1), 464-472.

[33] Klimek, M. (2001). Fractional sequential mechanics-models with symmetric fractional derivative. *Czechoslovak Journal of Physics*, *51*(12), 1348-1354.

[34] Merdan, M. (2010). A new applicaiton of modified differential transformation method for modeling the pollution of a system of lakes. *Selçuk Journal of Applied Mathematics, 11*(2), 27-40.

[35] Alkan, A. (2022). Improving Homotopy Analysis Method with An Optimal Parameter for Time-Fractional Burgers Equation. *Karamanoğlu Mehmetbey Üniversitesi Mühendislik ve Doğa Bilimleri Dergisi, 4*(2), 117-134.

[36] Wang, K., Liu, S. (2016). A new Sumudu transform iterative method for time-fractional Cauchy reaction-diffusion equation. *Springer Plus*, *5*(1), 865.

[37] Wazwaz, A. M. (1999). A reliable modification of Adomian decomposition method. *Applied Mathematics and Computation*, *102*(1), 77-86.

[38] Aslefallah, M., Abbasbandy, S., Yüzbaşi, Ş. (2023). Numerical Solution for a Class of Nonlinear Emden-Fowler Equations by Exponential Collocation Method. *Applications and Applied Mathematics: An International Journal (AAM)*, *18*(1), 10.

[39] Abdeljawad, T. (2015). On conformable fractional calculus. *Journal of computational and Applied Mathematics*, *279*, 57-66.

[40] Ala, V., Demirbilek, U., Mamedov, K. R. (2020). An application of improved Bernoulli sub-equation function method to the nonlinear conformable time-fractional SRLW equation. *AIMS Mathematics*, *5*(4), 3751-3761.

[41] Gözütok, U., Çoban, H., Sağıroğlu, Y. (2019). Frenet frame with respect to conformable derivative. *Filomat, 33*(6), 1541-1550.

[42] Shrinath, M., Bhadane, A. (2019). New conformable fractional Elzaki transformation: Theory and applications. *Malaya Journal of Matematik, 1*, 619-625.

[43] Ali, L., Shah, R., & Weera, W. (2022). Fractional View Analysis of Cahn–Allen Equations by New Iterative Transform Method. *Fractal and Fractional*, *6*(6), 293.

[44] Yasar, E., Giresunlu, I. B. (2016). The (G'/G, 1/G)-expansion method for solving nonlinear space-time fractional differential equations. *Pramana*, 87, 17.

[45] Esen, A., Yagmurlu, N. M., Tasbozan, O. (2013). Approximate analytical solution to time-fractional damped Burger and Cahn-Allen equations. *Appl. Math. Inf. Sci.*, 7, 1951.

[46] Jafari, H., Tajadodi, H., Baleanu, D. (2014). Application of a homogeneous balance method to exact solutions of nonlinear fractional evolution equations. *J. Comput. Nonlinear Dyn.*, 9, 021019-1.

[47] Hariharan, G., Kannan, K. (2009). Haar wavelet method for solving Cahn-Allen equation. *Appl. Math. Sci.*, 3, 2523–2533.

[48] Tascan, F., Bekir, A. (2009). Travelling wave solutions of the Cahn-Allen equation by using first integral method. *Appl. Math. Comput.*, 207, 279–282.

[49] Tariq, H., Akram, G. (2017). New traveling wave exact and approximate solutions for the nonlinear Cahn-Allen equation: Evolution of a nonconserved quantity. *Nonlinear Dyn.*, 88, 581–594.

[50] Bekir, A. (2012). Multisoliton solutions to Cahn-Allen equation using double exp-function method. *Phys. Wave Phenom.*, 20, 118–121.

[51] Guner, O., Bekir, A., Cevikel, A.C. (2015). A variety of exact solutions for the time fractional Cahn-Allen equation. *The European Physical Journal Plus*, 130, 1-13.